



**HAL**  
open science

## A new technique for the calculation and 3D visualisation of magnetic complexities on solar satellite images

O.W. Ahmed, R. Qahwaji, T. Colak, Thierry Dudok de Wit, S. Ipson

### ► To cite this version:

O.W. Ahmed, R. Qahwaji, T. Colak, Thierry Dudok de Wit, S. Ipson. A new technique for the calculation and 3D visualisation of magnetic complexities on solar satellite images. *The Visual Computer*, Springer Verlag, 2010, 26 (5), pp.385-395. 10.1007/s00371-010-0418-1 . insu-03388587

**HAL Id: insu-03388587**

**<https://hal-insu.archives-ouvertes.fr/insu-03388587>**

Submitted on 24 Feb 2022

**HAL** is a multi-disciplinary open access archive for the deposit and dissemination of scientific research documents, whether they are published or not. The documents may come from teaching and research institutions in France or abroad, or from public or private research centers.

L'archive ouverte pluridisciplinaire **HAL**, est destinée au dépôt et à la diffusion de documents scientifiques de niveau recherche, publiés ou non, émanant des établissements d'enseignement et de recherche français ou étrangers, des laboratoires publics ou privés.



UNIVERSITY of  
BRADFORD

## A New Technique for the Calculation and 3D Visualisation of Magnetic Complexities on Solar Satellite Images

Item Type	Article
Authors	Ahmed, Omar W.; Qahwaji, Rami S.R.; Colak, Tufan; Dudok De Wit, T.; Ipson, Stanley S.
Citation	Ahmed OW, Qahwaji RSR, Colak T, Dudok De Wit D and Ipson SS (2010) A New Technique for the Calculation and 3D Visualisation of Magnetic Complexities on Solar Satellite Images. Visual Computer. 26(5): 385-355.
Rights	(c) 2010 Springer Verlag. Full-text reproduced in accordance with the publisher's self-archiving policy.
Download date	24/02/2022 16:11:21
Link to Item	<a href="http://hdl.handle.net/10454/7600">http://hdl.handle.net/10454/7600</a>



---

# **The University of Bradford Institutional Repository**

<http://bradscholars.brad.ac.uk>

This work is made available online in accordance with publisher policies. Please refer to the repository record for this item and our Policy Document available from the repository home page for further information.

To see the final version of this work please visit the publisher's website. Access to the published online version may require a subscription.

**Link to original published version:** <http://dx.doi.org/10.1007/s00371-010-0418-1>

**Citation:** Ahmed OW, Qahwaji RSR, Colak T, Dudok De Wit D and Ipson S (2010) A New Technique for the Calculation and 3D Visualisation of Magnetic Complexities on Solar Satellite Images. *Visual Computer*. 26(5): 385-355.

**Copyright statement:** © 2010 Springer Verlag. Full-text reproduced in accordance with the publisher's self-archiving policy.

Editorial Manager(tm) for The Visual Computer  
Manuscript Draft

Manuscript Number:

Title: A New Technique for the Calculation and 3D Visualisation of Magnetic Complexities on Solar Satellite Images

Article Type: Special Issue Article

Keywords: Active Regions, Solar Disk, Solar Flares, Magnetic Complexity, Energy, Satellite Images, 3D Sun.

Corresponding Author: Mr Omar Wahab Ahmed, BSc

Corresponding Author's Institution: University of Bradford

First Author: Omar Wahab Ahmed, BSc

Order of Authors: Omar Wahab Ahmed, BSc; Rami Qahwaji, BSc, MSc, Ph.D.; Tufan Colak, BSc, MSc, Ph.D. ; Thierry DUDOK DEWIT, M.A., Ph.D., Prof; Stan Ipson, BSc, Ph.D.

# A New Technique for the Calculation and 3D Visualisation of Magnetic Complexities on Solar Satellite Images

O. W. AHMED<sup>1</sup>, R. QAHWAJI<sup>1</sup>, T. COLAK<sup>1</sup>, T. DUDOK DE WIT<sup>2</sup> and S. IPSON<sup>1</sup>

<sup>1</sup>*School of Computing, Informatics and Media, University of Bradford, Bradford BD7 1DP, UK*

<sup>2</sup>*LPC2E, University of Orléans, 3A Av. de la Recherche Scientifique, 45071 Orleans cedex 2, France*

E-mails: [O.W.Ahmed@bradford.ac.uk](mailto:O.W.Ahmed@bradford.ac.uk), [r.s.r.qahwaji@bradford.ac.uk](mailto:r.s.r.qahwaji@bradford.ac.uk), [t.colak@bradford.ac.uk](mailto:t.colak@bradford.ac.uk), [ddwit@cns-orleans.fr](mailto:ddwit@cns-orleans.fr), [S.S.Ipson@Bradford.ac.uk](mailto:S.S.Ipson@Bradford.ac.uk).

Original work presented in CyberWorlds 2009 Conference

**Abstract:** In this paper, we introduce two novel models for processing real-life satellite images to quantify and then visualise their magnetic structures in 3D. We believe this multidisciplinary work is a real convergence between image processing, 3D visualization and solar physics. The first model aims to calculate the value of the magnetic complexity in active regions and the solar disk. A series of experiments are carried out using this model and a relationship has been indentified between the calculated magnetic complexity values and solar flare events. The second model aims to visualise the calculated magnetic complexities in 3D colour maps in order to identify the locations of eruptive regions on the Sun. Both models demonstrate promising results and they can be potentially used in the fields of solar imaging, space weather and solar flare prediction and forecasting.

**Keywords:** *Active Regions, Solar Disk, Solar Flares, Magnetic Complexity, Energy, Satellite Images, 3D Sun.*

Abbreviations MDI: Michelson Doppler Imager; SOHO: Solar and Heliospheric Observatory; ESA: European Space Agency; NASA: National Aeronautics and Space Administration; NGDC: National Geophysical Data Center; GIF: Graphic Interchange Format; NOAA: National Oceanic and Atmospheric Administration; OpenGL: Open Graphics Library; ASAP: Automated Solar Activity Prediction.

# 1. Introduction

Research and interest in the field of space weather and solar activities is growing because of the significance of their potential impact on human lives and activities. The term space weather is applied to the space environment around the Earth and all the way to the Sun. Space weather is defined as the “conditions on the Sun and in the solar wind, magnetosphere, ionosphere, and thermosphere that can influence the performance and reliability of space-born and ground-based technological systems and can endanger human life or health. Adverse conditions in the space environment can cause disruption of satellite operations communications, navigation, and electricity power distribution grids, leading to a variety of socioeconomic losses” [1] [2] [3]. In the past, few solar activities have affected the Earth and caused notable damage. In March 1989, power grids in north-east Canada collapsed during a great geomagnetic storm which left millions of people without electricity [4]. Another large event occurred during the end of October beginning of November 2003 period, when the largest ever recorded X-ray flare occurred, known as the Halloween solar storm. It damaged 28 satellites, knocking two out of commission, causing airplane routes to be diverted and power failures in Sweden and other countries [5] [6]. Thus, there is an urgent need to develop preventative measures capable of reducing the risks associated with space weather events, by introducing either a system design or efficient warning and prediction systems [3] [7]. This will allow industries at risk to take preventative measures to avoid or mitigate the consequences of these events. Space weather and solar activities are both directly influenced by the Sun. As such it is important to study the Sun and its activities in order to have a good understanding of its influence on space weather [1]. Solar flares are the most remarkable solar activities which drive space weather and affect the terrestrial environment as they spew vast quantities of radiation and charged particles into space [8] [9]. Flares are defined as sudden, rapid, and intense variations in brightness that occurs when the magnetic energy that has built up in the solar atmosphere is suddenly released, over a period lasting from minutes to hours. Flares emit strong radiation such as radio waves, X-rays and gamma rays, and energetic particles (protons and electrons) [10]. Solar flares mostly occur in active regions, as such, it is important to study active regions in order to have a good understanding of flares. Active regions are regions on the Sun usually form with sunspots, and they are studied in order to forecast solar activities. Solar active regions are associated with particularly strong and complex magnetic

1  
2  
3  
4 fields, which emerge through the photosphere into the chromosphere and corona. This creates  
5 suitable conditions for the release of enormous amounts of energy in the form of solar flares.  
6  
7 Understanding this energy is important as it aids the prediction of solar eruptions, such as solar  
8 flares as well as other solar activities.  
9

10  
11 The work presented here demonstrates recent developments in our ongoing efforts to design a  
12 web-based, automatic and real-time system for predicting and forecasting solar flares. Two new  
13 models are introduced in this paper. Both models were executed using daily solar images  
14 captured by MDI (Michelson Doppler Imager) instrument on board of the SOHO (Solar &  
15 Heliospheric Observatory) satellite [11]. The first model introduces a method to calculate the  
16 magnetic complexity in active regions and in the solar disk for the purpose of solar flare  
17 prediction. The magnetic complexity calculation model is based on the famous physical Ising  
18 model [12]. The Ising model has been modified to fit the nature of this application. The method  
19 introduced here is the latest updated version, which is better fitted to imitate the property of the  
20 magnetic fields connections in active regions. More details about the original Ising model and  
21 the earlier models can be found in our previous publications [13] [14]. The magnetic  
22 complexities were calculated for number of different groups of active regions and solar disk  
23 samples. Then, their values were plotted against flare events that have occurred during the same  
24 period and location. This has revealed a clear relationship between the recorded magnetic  
25 complexities and flare events. The second model visualise the solar disk, active regions, and the  
26 calculated magnetic complexity in 3D colour maps. This model reconstructs the studied  
27 magnetogram image and represents it for 3D view. Also the model can view 3D colour map of  
28 active regions according to their polarity or to the calculated magnetic complexity. This can  
29 identify the potentially eruptive regions. The models proposed in this paper offer a new approach  
30 to observe solar images for the purpose of solar flare prediction and forecasting.  
31  
32

33  
34  
35  
36  
37  
38  
39 This paper is organized as follows: solar data sources are introduced in section 2. Section 3  
40 introduces the magnetic complexity calculation model and how it has been used to calculate the  
41 magnetic complexity in active regions and in the solar disk. Section 4 describes the 3D  
42 visualisation model. Finally, the conclusion and future work is discussed in section 5.  
43  
44  
45  
46  
47  
48  
49  
50  
51  
52  
53  
54  
55  
56  
57  
58  
59  
60  
61  
62  
63  
64  
65

## 2. Solar Data

### 2.1. Satellite Images

SOHO/MDI magnetogram images have been used in this work. These images are captured by MDI (Michelson Doppler Imager) instrument, which is on board the SOHO (Solar and Heliospheric Observatory) satellite. SOHO is a project of international cooperation between ESA (European Space Agency) and NASA (National Aeronautics and Space Administration). SOHO/MDI magnetogram images are available publically online<sup>1</sup> in GIF format (Graphic Interchange Format). The magnetogram images record the line-of-sight components of the magnetic fields on the solar disk [15] as shown in Figure 1. These images are used in this work because they show the strength and location of the magnetic fields on the Sun, which makes them well suited for magnetic complexity calculation method. There are around 15 SOHO/MDI magnetogram images available per day. Every two images are separated by approximately a 90 minute gap. This is beneficial for the use of the proposed models in terms of tracking the changes in the magnetic complexity values of the active regions in relation to flare occurrence. MDI magnetogram images are in grayscale, where pixel intensities range from 0-255. The minimum pixel intensity value represents black, while the maximum pixel intensity value represents white. Each colour represents the magnetic polarity distribution on the solar disk. The gray areas indicate regions with minimum magnetic energies, while the black and white regions indicate strong magnetic fields. The black regions indicate “south” magnetic polarity (pointing towards the Sun), while white regions indicate “north” magnetic polarity (pointing outwards) [16].

### 2.2. NGDC Flare Catalogues

Solar flare catalogues obtained from the National Geophysical Data Center (NGDC) have also been used in this work. These catalogues are available for public access online<sup>2</sup>. NGDC holds one of the most comprehensive public databases for solar features and activities records from

---

<sup>1</sup> [http://soi.stanford.edu/production/mag\\_gifs.html](http://soi.stanford.edu/production/mag_gifs.html)

<sup>2</sup> [ftp://ftp.ngdc.noaa.gov/STP/SOLAR\\_DATA](ftp://ftp.ngdc.noaa.gov/STP/SOLAR_DATA)



1  
2  
3  
4 several observatories around the world. The NGDC flare events catalogues include full details  
5 about flares, such as flare's date, time, location, classification, intensity and NOAA number.  
6 Flares are classified according to their X-ray brightness as follows: A, B, C, M, or X. A and B  
7 flares are the weakest, while M and X flares are the strongest. C flares are weak in comparison to  
8 M and X flares and they could have few noticeable impacts on space weather. M and X flares are  
9 more related to major impacts on space weather, especially X flares. The NOAA number is a  
10 unique number, for each active region, given by the National Oceanic and Atmospheric  
11 Administration (NOAA). Using the NOAA number, flares can be assigned to the active regions  
12 that they have originated from. However, not all of the recorded flares are assigned to a NOAA  
13 number. This could be related to the difficulty of assigning a flare to the right active region,  
14 especially during solar maximum when in some scenarios active regions could be attached to or  
15 in a group of complex active regions, or the recorded flare might have occurred on the far side of  
16 the Sun.  
17  
18  
19  
20  
21  
22  
23  
24  
25  
26  
27

### 28 **3. The Magnetic Complexity Model**

29  
30  
31  
32 The idea of the magnetic complexity calculation model is based on the relationship between the  
33 energy stored in the magnetic fields of active regions and flares erupting from these regions. The  
34 magnetic complexity calculation model is derived from the Ising model. The Ising model is used  
35 for the analysis of magnetic interactions and structures of ferromagnetic substances [12]. This  
36 model allows for the simplification of complex interactions, since it has been successfully  
37 employed in several areas of science. The Ising model has been applied to many physical  
38 systems such as: magnetism, binary alloys, and the liquid-gas transition [17]. The model was  
39 also used in biology to model neural networks, flocking birds and beating heart cells [18] [19]  
40 [20]. Between 1969 and 1997, more than 12,000 papers were published using this model in  
41 different applications, which shows the importance and potential of this model [21]. For the first  
42 time, the Ising model has been modified and then applied to model the properties of magnetic  
43 fields formation in active regions and calculate the magnetic complexity of active regions. More  
44 details about the original Ising model and the first attempts of the modified model can be  
45 obtained in our previous publications [13] [14]. However, further modifications have been  
46 applied to the model since the first attempts in modifying the Ising model. To avoid confusion, it  
47  
48  
49  
50  
51  
52  
53  
54  
55  
56  
57  
58  
59  
60  
61  
62  
63  
64  
65

1  
2  
3  
4 is worth mentioning that the “magnetic complexity” have also been declared as the “energy” in  
5  
6 our previous publications. However, the new model imitates the magnetic configurations in  
7  
8 active regions, which are the key factor in flare occurrence, to provide more accurate results. The  
9  
10 calculated values should provide a new way to indicate the flaring and non-flaring active regions,  
11  
12 or even flare classifications. Also, the magnetic complexity calculation model has been applied  
13  
14 to calculate the overall magnetic complexity on the solar disk. This will provide a measure of the  
15  
16 overall magnetic activities on the front-side of the Sun, and therefore can be an important  
17  
18 indicator for flare occurrences in general.

19 SOHO/MDI magnetogram images are used in this work. The magnetogram images are processed  
20  
21 and represented in a 2D grid, according to pixel intensities. Each pixel value in the magnetogram  
22  
23 image is represented in the grid as follows:

- 24 • Pixel intensity values between 0 and 30 represent the *black* areas in the image. These areas  
25  
26 indicate a south magnetic polarity and are represented as -1 in the grid.
- 27 • Pixel intensity values between 230 and 255 represent the *white* areas in the image. These  
28  
29 areas indicate a north magnetic polarity and are represented as +1 in the grid.
- 30 • Pixel intensity values between 31 and 229 represent the *gray* areas in the image. These areas  
31  
32 indicate minimum magnetic energies and are represented as 0 in the grid.

33  
34  
35 The magnetic complexity is calculated using Equation 1, which only takes the following values  
36  
37 as an input: +1 and -1. In the equation,  $S_i$  represents the north polarity areas only (+1), and  $S_j$   
38  
39 represents the south polarity areas only (-1). The magnetic fields in active regions loop from the  
40  
41 positive magnetic fields to the negative magnetic fields. This property has been applied to the  
42  
43 calculation method. The multiplication goes only from the values representing the positive  
44  
45 magnetic fields ( $S_i = +1$ ) to the negative magnetic fields ( $S_j = -1$ ), ignoring the weak polarity  
46  
47 areas (0) as shown in Figure 2, taking into consideration the distance ( $d$ ) between the interacting  
48  
49 spins.  $N$  is the number of the total spins (the size of the 2-D grid).  $E$  is the total energy or the  
50  
51 magnetic complexity, and it is unit-less.

$$E = - \sum_{i,j}^N \frac{S_i S_j}{d^2} \quad (1)$$

### 3.1. Calculating the Magnetic Complexity in Active Regions

A number of image processing techniques are applied to the MDI magnetogram images, prior to calculating the magnetic complexity in active regions. These procedures are summarized as follows:

- MDI magnetograms record the line-of-sight component of the magnetic fields on the solar disk. In this work it is important to have the magnetic fields of the MDI magnetogram images represented accurately. Due to the projection effect, it was noticed that active regions located near the solar limb were distorted and it was difficult to observe and record the line-of-sight component of the magnetic fields in these regions. Data far from the solar disk is less reliable because of the observing angle correction factor [22]. This leads to inaccurate representations of the active regions located near the solar limb. In order to resolve this problem, the MDI magnetogram image has been re-mapped using the method conducted in [23]. The magnetogram image is re-mapped from Heliocentric Cartesian coordinates to Carrington Heliographic coordinates. Then, the solar disk is shifted so the investigated active region located in the center of the image. This is done by selecting the solar disk image which has the active region under investigation located on around zero longitude, in order to use the active region time and location information as a reference point in the shifting process. Finally, the solar disk is re-mapped again to Heliocentric Cartesian coordinates. The resulting image shows the solar disk is shifted and the active region under investigation is located in the center of the image, as shown in Figure 3.
- Despite the remapping process, it was noticed that several active regions located near the solar limb were still distorted. Therefore, active regions located above  $45^\circ$  from the center of the solar disk were discarded.
- Most of the MDI magnetogram images used in this work included a random noise. Hence, it was necessary to apply an image filtering method to reduce the noise in these images. A  $(3 \times 3)$  Median filter was applied for this purpose. This filter is quite popular due to the excellent noise reduction capability it can provide for certain types of random noise [24]. An example of an active region image before and after applying the median filter is shown in Figure 4. This means that the new algorithm is more likely to achieve reliable results because better quality images are used.

- The active region under investigation is detected and cropped from the magnetogram image in order to calculate the magnetic complexity using Equation 1, as explained previously.

A number of active regions candidates selected from different period of times, during solar minimum and solar maximum, were experimented with. The NOAA number and date of these active regions are: (10308 08/03/2003-18/03/2003), (10314 13/03/2003-18/03/2003), (10365 20/05/2003-01/06/2003), (10482 17/10/2003-27/10/2003), (10484 17/10/2003-30/10/2003), (10486 25/10/2003-03/11/2003), (10488 25/10/2003-03/11/2003), (10507 19/11/2003-30/11/2003), (9393 24/03/2001-02/04/2001), (10956 17/05/2007-21/05/2007). The calculated magnetic complexity values for each of the investigated active regions were compared to the flares that erupted from the same region, and they are both plotted against time. As a conclusion, these active regions have been classified according to their magnetic complexity values as follows:

1. *Non-Flaring Active Regions, Magnetic Complexity < 500.* These active regions were holding very low energy and occasionally were accompanied with few B flares. This can be seen in region 482 as shown in Figure 5.
2. *Steady Increase Regions, 500 < Magnetic Complexity < 10,000.* Active regions within this range usually had a gradual increase in their energy. Flares of type C, M and X erupted as the energy increased. Also, it has been noticed that flares occurred as groups separated by approximately 10 hours. This can be seen in region 365, shown in Figure 6.
3. *Highly Energetic Regions, Magnetic Complexity > 10,000.* These active regions were holding very high energy, accompanied by high number of flares of type C, M and X. Also, it has been noticed that erupted flares were separated by short time intervals. This can be seen in region 9393, shown in Figure 7.

Also, it was noticed that the number of flares increases as the energy (magnetic complexity) increases. As a conclusion, these outcomes show a good indication of the state of active regions in relation to flare occurrences.

### **3.2. Calculating the Magnetic Complexity in the Solar Disk**

On many occasions, especially during the solar maximum when the number of sunspots and active regions is high, it is difficult to assign some of the erupted flares to the active regions that they originated from. This is because either there are groups of complex active regions adjacent

1  
2  
3  
4 to one other, or the flare might have occurred on the backside of the Sun. Therefore it is  
5 important to have an indicator to reflect the overall status of the solar disk. Based on this, we are  
6 introducing a new technique to calculate the solar disk magnetic complexity. The ideology of  
7 this method is comparable to the solar cycle and it can be used to determining the overall solar  
8 activities on the Sun, which could be useful for flare prediction. A summary of the method's  
9 processes is described below:

- 15 • The MDI magnetogram image is filtered using the Median filter. This is similar to the  
16 approach explained in section 3.1.
- 17 • The solar disk is detected in order to exclude the black areas around the disk.
- 18 • The magnetic complexity of the solar disk is calculated using Equation 1, as explained  
19 previously.

20 This method has been experimented using MDI magnetogram images over a number of months;  
21 April 2001, June 2003, March 2001, March 2003, May 2003, May 2005, May 2007, November  
22 2003, October 2003 and October 2004. The calculated values have been plotted against flares  
23 that occurred during the same period. A clear relationship can be noticed between both curves in  
24 the plots. As a conclusion, it was noticed that the number of flare events increases with the  
25 increase of the solar disk magnetic complexity (energy), and vice versa. Some of the results are  
26 shown in Figure 8, Figure 9, and Figure 10.

## 37 38 **4. 3D Visualisation of the Magnetic Complexities on the Solar** 39 **Disk**

40  
41 A new tool has been developed using OpenGL (Open Graphics Library) program to visualise the  
42 solar disk, active regions, and the calculated magnetic complexity in terms of 3D colour maps.  
43 The 3D colour maps offer a new approach to visualise active regions across the solar disk  
44 according to their polarities or to their magnetic complexities. This is very useful in terms of  
45 identifying the potentially eruptive areas on the solar disk. Viewing the Sun in 3D is very  
46 advantageous in comparison with the regular 2D images, as it offers different viewing experience  
47 i.e. zooming in/out and navigating through the Sun and solar activities. Also it offers a better  
48 viewing of solar activities located near the solar limb. This tool is very constructive, it offers a  
49  
50  
51  
52  
53  
54  
55  
56  
57  
58  
59  
60  
61  
62  
63  
64  
65

1  
2  
3  
4 new approach in visualising and investigating solar activities, and it can be used effectively in  
5 the field of space weather research.

6  
7  
8 The OpenGL based tool reads a text file as an input, which includes the properties of the  
9 extracted features from the magnetogram image under investigation. The steps that have been  
10 undertaken to extract the required features are explained below:

- 11 • The SOHO/MDI magnetogram image is converted to the Carrington Heliographic  
12 coordinates. Using the method employed in [23].
- 13 • Active regions are detected from the Heliographic coordinate image, using intensity  
14 filtering. The intensity filtering threshold value  $T_f$  for each image is found automatically  
15 using Equation 2, where,  $\mu$  is the mean,  $\sigma$  represents the standard deviation, and  $\alpha$  is a  
16 constant that is determined empirically based on the type of the features to be detected and  
17 the images.

$$18 \quad T_f = \mu \pm (\sigma \times \alpha) \quad (1)$$

19  
20  
21  
22  
23  
24  
25  
26  
27  
28  
29  
30 The value of the first threshold is determined using Equation (2) with the plus (+) sign and  $\alpha$   
31 equal to 2. All pixels that have intensity values larger than this threshold are marked as  
32 active regions with north polarity. In the same manner, the second threshold is determined  
33 using Equation (2) with the minus (-) sign and  $\alpha$  equals to 2. Any pixel with intensity value  
34 less than this threshold is marked as active regions with south polarity.

- 35 • After detecting the pixels that represent active regions, the magnetic complexity values are  
36 calculated using Equation 1 and represented as colours ranging from red to green. Where red  
37 represents the highest complexity and green represents the lowest complexity.
- 38 • Then using Equation (3), 3D Cartesian coordinates of each pixel is calculated. In this  
39 equation,  $B$  is equal to latitude,  $L$  is equal to longitude of the detected solar pixel and  $r$  is  
40 equal to the radius of the solar disk that the new data is mapped to.

$$41 \quad x = r \sin (B) \cos (L)$$

$$42 \quad y = r \sin (B) \sin (L) \quad (3)$$

$$43 \quad z = r \cos (B)$$

44  
45  
46  
47  
48  
49  
50  
51  
52  
53  
54  
55  
56  
57  
58  
59  
60  
61  
62  
63  
64  
65

- All the calculated 3D coordinates of the pixels are recorded to text files along with their colour values and visualised using the OpenGL based 3D tool.

This tool has been tested on the same active regions that had their magnetic complexities values investigated previously in section 3.1. The results of this model are shown in Figure 11 in three groups: (A), (B), and (C), and they can be compared to the previous results, which discussed in section 3.1 and presented in Figure 5, 6, 7 respectively. Each group in Figure 11 consists of four images. The first is a magnetogram image. The second image is a 3D colour map of the solar disk which shows the active regions as white/gray areas, where white represents the north polarity regions, and gray represents the south polarity regions. The third image is a 3D colour map of the solar disk which shows the high magnetic complexity areas represented as red colour and the low magnetic complexity areas represented as green colour. The red coloured areas indicate a potential flare eruption location, while the green coloured areas indicate quite locations. The fourth image is a 3D wired view of the solar disk, which shows another view of the third image.

## 5. Conclusion and Future Work

Two new models have been presented in this paper. The first calculates the magnetic complexity in active regions and the solar disk. This model is based on the famous physical Ising model, which has been modified to suit the properties of this application. The second is to visualise the solar disk, active regions, and the calculated magnetic complexity in 3D colour maps. SOHO/MDI magnetogram images are used for this research. Both models have been developed with C++ programming language and OpenGL software for 3D applications. Also they have been tested on different groups of samples selected randomly from different time periods. The obtained results reveal a relationship between the calculated magnetic complexities in active regions and the solar disk with flares. Also, the calculated magnetic complexity values have been represented in a 3D model in order to visualise the flaring regions on the solar disk. These models demonstrate very significant findings and can be useful tools for solar imaging, space weather and applied imaging in general.

The aim of our research is to develop an automatic, real-time, and web-based system for solar flare forecasting. Currently, the models presented here can perform in real time. However,

1  
2  
3  
4 further work will be carried out on large amount of data in order to establish the exact correlation  
5 between the calculated magnetic complexities and flares in order to evaluate the capability of the  
6 model to accurately predict flare classes. This will be investigated using statistical or machine  
7 learning methods. Also, the magnetic complexity model will be integrated with ASAP  
8 (Automated Solar Activity Prediction). ASAP is an automated solar forecasting system which  
9 predict flares based on the sunspot's McIntosh classification and area [25] [26], available online<sup>3</sup>.  
10 This step will enable us to determine number of solar activities parameters which are related to  
11 flare events, such as: *sunspot's McIntosh classifications, sunspots' area, active region's*  
12 *magnetic complexity, and solar disk magnetic complexity*, which can provide better flare  
13 prediction. Finally, the 3D visualisation model will be updated so it can be used to reconstruct  
14 and represent other solar images i.e. SOHO/MDI Continuum images, EIT images, etc., and  
15 represent the solar features that are presented in these images.  
16  
17  
18  
19  
20  
21  
22  
23  
24  
25  
26

## 27 References

- 28  
29  
30 [1] M. Moldwin, *An Introduction to Space Weather*. Los Angeles, 2008.  
31 [2] O. o. t. F. C. f. Meteorology, "National Space Weather Program Strategic Plan," 1995.  
32 [3] H. Koskinen, E. Tanskanen, R. Pirjola, and A. Pulkkinen, "SPACE WEATHER EFFECTS  
33 CATALOGUE," *ESA Space Weather Study (ESWS)*, January 2 2001.  
34 [4] N. R. C. Committee on the Societal and Economic Impacts of Severe Space Weather Events: A Workshop,  
35 *Severe Space Weather Events--Understanding Societal and Economic Impacts:A Workshop Report*. Washington, :  
36 THE NATIONAL ACADEMIES PRESS, 2008.  
37 [5] S. T. Online, "Halloween Storm Surge Shocks Earth." vol. 2008: Space Today Online, 2004.  
38 [6] R. Qahwaji and T. Colak, "Automatic Prediction of Solar Flares using Machine Learning: Practical Study  
39 on the Halloween Storm," in *IEEE conference on Recent Advances in Space Technologies* Istanbul: IEEE, 2007.  
40 [7] J. Feynman and S. B. Gabriel, "On Space Weather Consequences and Predictions," *J Geophys. Res.*, vol.  
41 105, pp. 10 543- 10 564, 2000.  
42 [8] M. Pick, C. Lathuillere, and J. Lilensten, "Ground Based Measurements," *ESA Space Weather Programme*  
43 *Feasibility Studies*, 2001.  
44 [9] D. Lenz, "Understanding and Predicting Space Weather," *The Industrial Physicist*, pp. 18-21, 2004.  
45 [10] S. T. Dispatch, "Internet Space Weather And Radio Propagation Forecast Course," Solar Terrestrial  
46 Dispatch, 1996-2001.  
47  
48  
49  
50  
51  
52  
53  
54  
55  
56

---

57  
58  
59 <sup>3</sup> <http://spaceweather.inf.brad.ac.uk>  
60  
61  
62  
63  
64  
65



- 1  
2  
3  
4 [11] P. H. Scherrer, R. S. Bogart, R. I. Bush, J. T. Hoeksema, A. G. Kosovichev, J. Schou, W. Rosenberg, L.  
5 Springer, T. D. Tarbell, A. Title, C. J. Wolfson, I. Zayer, and T. M. E. Team, "The Solar Oscillations Investigation -  
6 Michelson Doppler Imager," *Solar Physics*, vol. 162, pp. 129-188, December 1995.  
7  
8 [12] E. Ising, "Beitrag zur Theorie des Ferromagnetismus," *Z. Phys*, vol. 31, pp. 3-4, 1925.  
9  
10 [13] O. Ahmed, R. Qahwaji, T. Colak, T. Dudok De Wit, and S. Ipson, "A New Method for Processing Solar  
11 Images to Calculate the Magnetic Energies Associated with Active Regions," in *Systems, Signals and Devices, 2008.*  
12 *IEEE SSD 2008. 5th International Multi-Conference on*, 2008, pp. 1-5.  
13  
14 [14] O. Ahmed, R. Qahwaji, T. Colak, T. Dudok De Wit, and S. Ipson, "Applying a Modified Ising Algorithm to  
15 Calculate the Energy of Solar Active Regions in Solar Images," in *Communications, Computers and Applications,*  
16 *2008. MIC-CCA 2008. Mosharaka International Conference on*, Amman, 2008, pp. 43-48.  
17  
18 [15] S. NetLinks, "Tracking the Movement of Sunspots," Science NetLinks.  
19  
20 [16] K. R. Lang, *Sun, Earth and Sky*: Springer, 1995.  
21  
22 [17] J. P. Sethna, "Statistical Mechanics: Entropy, Order Parameters, and Complexity," OXFORD, 2007.  
23  
24 [18] Rowe GW and T. LE, "A thermodynamic theory of codon bias in viral genes," *J Theor Biol*, vol. 101, pp.  
25 171-203, 1983.  
26  
27 [19] I. A. P. C, and P. F, "Evidence for nonrandom hydrophobicity structures in protein chains," *Proc Natl Acad*  
28 *Sci USA* vol. 93, pp. 9533-9538, 1996.  
29  
30 [20] R. J. Ahsan A, Bruinsma R, "Elasticity theory of the B-DNA to S-DNA transition," *Biophys J*, vol. 74, pp.  
31 132-137, 1998.  
32  
33 [21] S. T. Wierzchon, "Ising Model," E. W. Weisstein, Ed.: WOLFRAM RESEARCH, 1996-2007.  
34  
35 [22] M. J. Knoll, K.D. Leka, G. Barnes, "Statistical Prediction of Solar Flares Using Line of Sight Magnetogram  
36 Data," 31 July 2008.  
37  
38 [23] T. Colak and R. Qahwaji, "Automated McIntosh-Based Classification of Sunspot Groups Using MDI  
39 Images," *Solar Physics*, vol. 248, pp. 277-296, 2008.  
40  
41 [24] R. C. Gonzalez and R. E. Woods, *Digital Image Processing*.  
42  
43 [25] R. Q. T. Colak, "ASAP: A Hybrid Computer Platform Using Machine Learning and Solar Imaging for  
44 Automated Prediction of Significant Solar Flares," *SPACE WEATHER*, 2008.  
45  
46 [26] T. C. R. Qahwaji, "Automatic Detection and Verification of Solar Features," *International Journal of*  
47 *Imaging Systems Technology*, vol. 15, pp. 199-210, 2005.  
48  
49  
50  
51  
52  
53  
54  
55  
56  
57  
58  
59  
60  
61  
62  
63  
64  
65

1  
2  
3  
4  
5  
6  
7  
8  
9  
10  
11  
12  
13  
14  
15  
16  
17  
18  
19  
20  
21  
22  
23  
24  
25  
26  
27  
28  
29  
30  
31  
32  
33  
34  
35  
36  
37  
38  
39  
40  
41  
42  
43  
44  
45  
46  
47  
48  
49  
50  
51  
52  
53  
54  
55  
56  
57  
58  
59  
60  
61  
62  
63  
64  
65

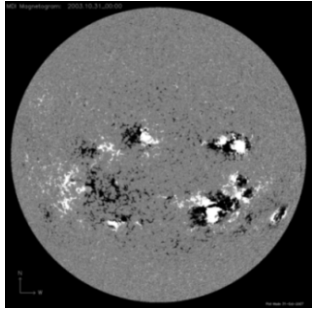


Figure 1. SOHO/MDI Magnetogram Image.

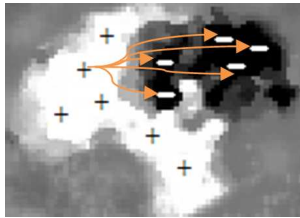


Figure 1. A sample of an active region showing the interaction between opposite polarity areas according to the magnetic complexity model. Each spin within the white area (+) will be multiplied by all the spins in the black area (-).

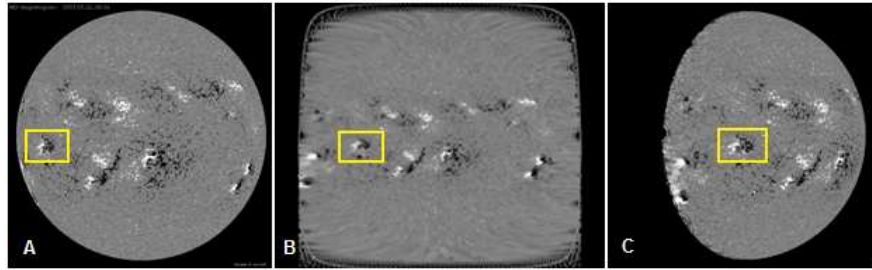
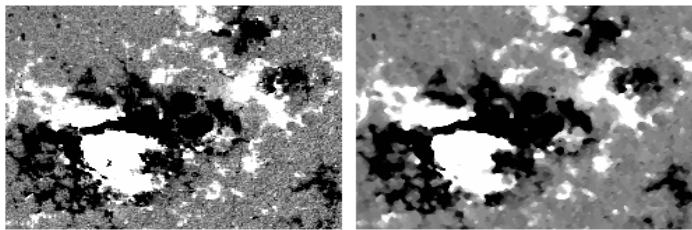


Figure 3. The three images above shows the re-mapping stages and how it affects an investigated region. Image date: 2003.05.22 06:24. Region NOAA number: 365. (A) The original magnetogram image in Heliocentric Cartesian coordinates. (B) The solar disk represented in Carrington Heliographic coordinates. (C) The solar disk re-mapped and represented in Heliocentric Cartesian coordinates, showing the active regions under investigation near the centre.



NOAA 10486 2003.10.30 00.00

Figure 4. An active region before (Left) and after (Right) applying the  $3 \times 3$  Median filter.

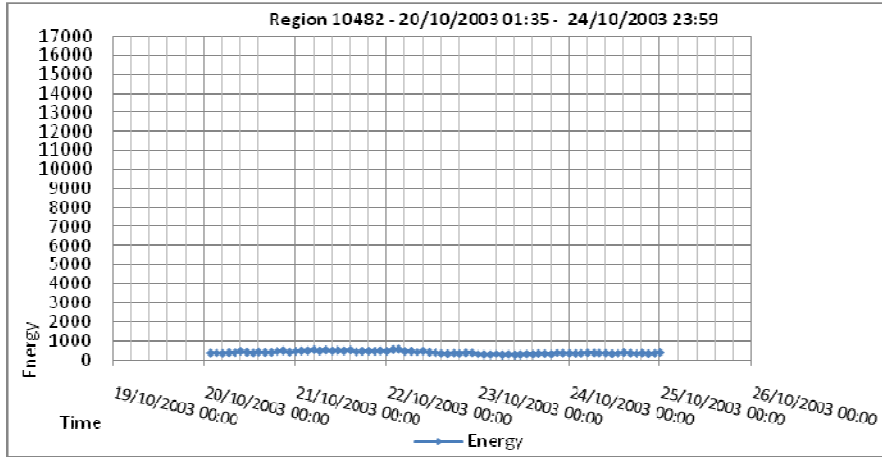


Figure 5. The curve represents the energy (Magnetic Complexity) of active region 482. Very low energy and no flares were recorded within the region.

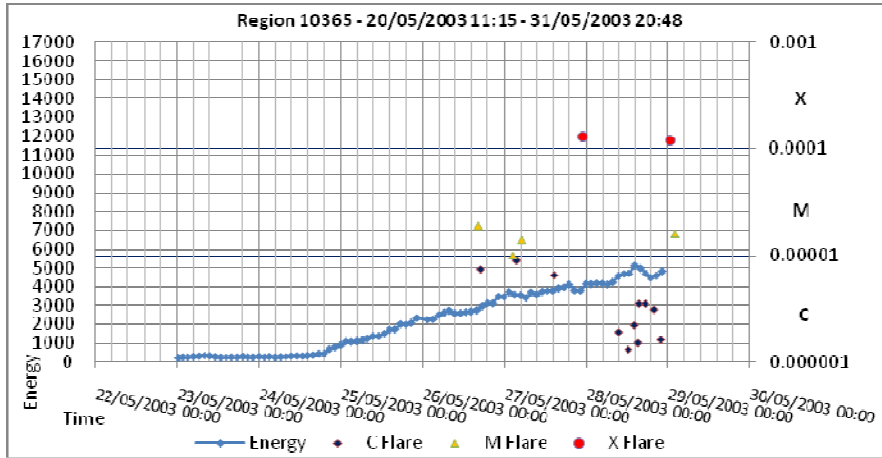


Figure 6. The curve represents the energy (Magnetic Complexity) of active region 365. A gradual build up in energy with flares occurred as groups separated by a period of time.

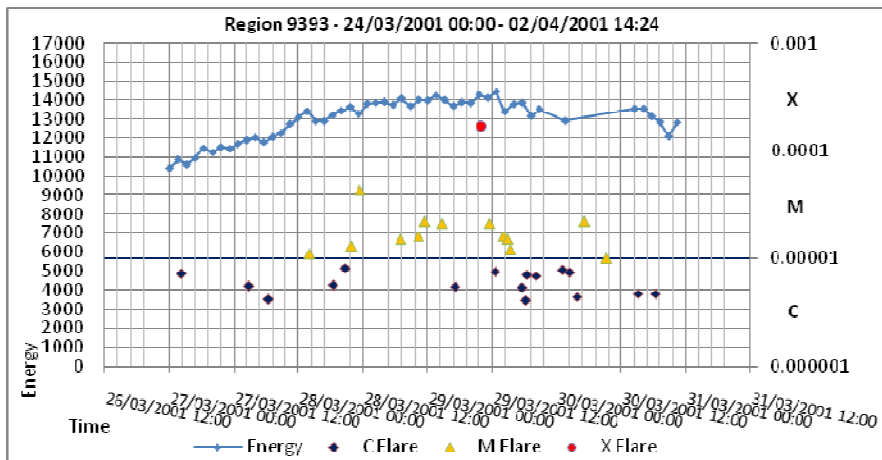


Figure 7. The curve represents the energy (Magnetic Complexity) of active region 9393. The energy is very high, accompanied by a high number of flares with short time intervals.

1  
2  
3  
4  
5  
6  
7  
8  
9  
10  
11  
12  
13  
14  
15  
16  
17  
18  
19  
20  
21  
22  
23  
24  
25  
26  
27  
28  
29  
30  
31  
32  
33  
34  
35  
36  
37  
38  
39  
40  
41  
42  
43  
44  
45  
46  
47  
48  
49  
50  
51  
52  
53  
54  
55  
56  
57  
58  
59  
60  
61  
62  
63  
64  
65

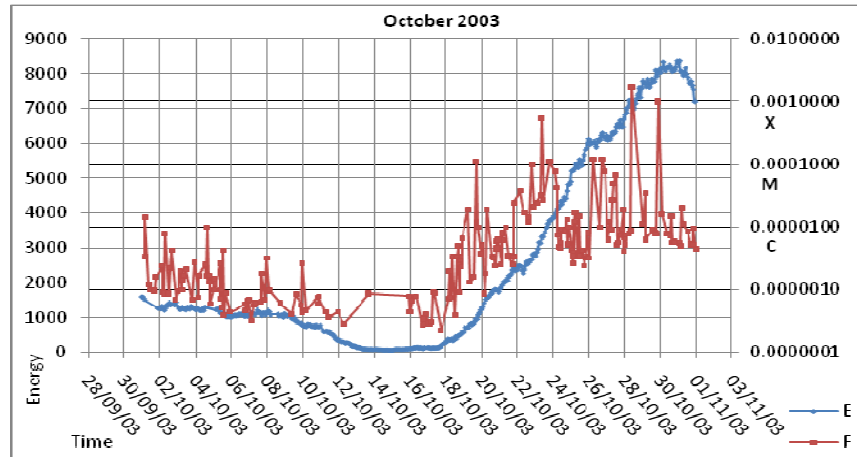


Figure 8. This plot shows the solar disk energy (Magnetic Complexity) and flares which occurred in October 2003.

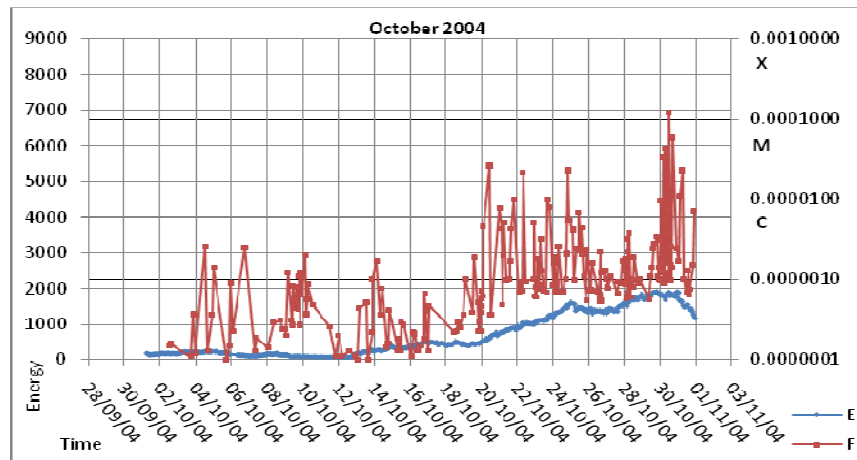


Figure 9. This plot shows the solar disk energy (Magnetic Complexity) and flares which occurred in October 2004.

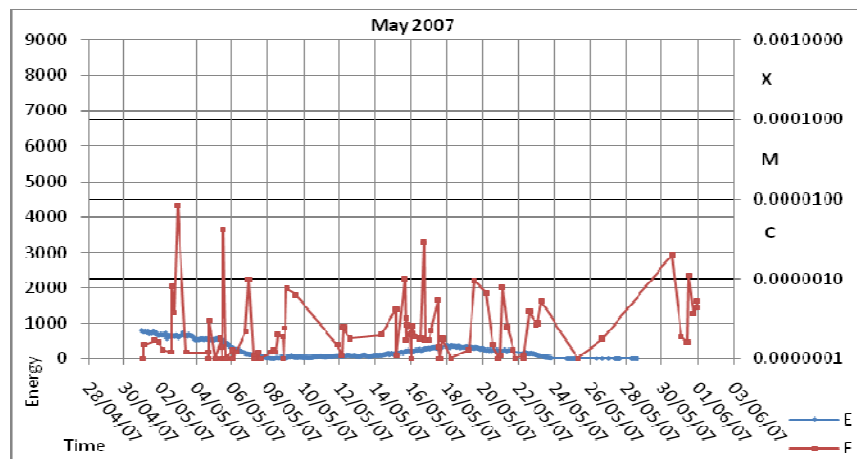


Figure 10. This plot shows the solar disk energy (Magnetic Complexity) and flares which occurred in May 2007.

1  
2  
3  
4  
5  
6  
7  
8  
9  
10  
11  
12  
13  
14  
15  
16  
17  
18  
19  
20  
21  
22  
23  
24  
25  
26  
27  
28  
29  
30  
31  
32  
33  
34  
35  
36  
37  
38  
39  
40  
41  
42  
43  
44  
45  
46  
47  
48  
49  
50  
51  
52  
53  
54  
55  
56  
57  
58  
59  
60  
61  
62  
63  
64  
65

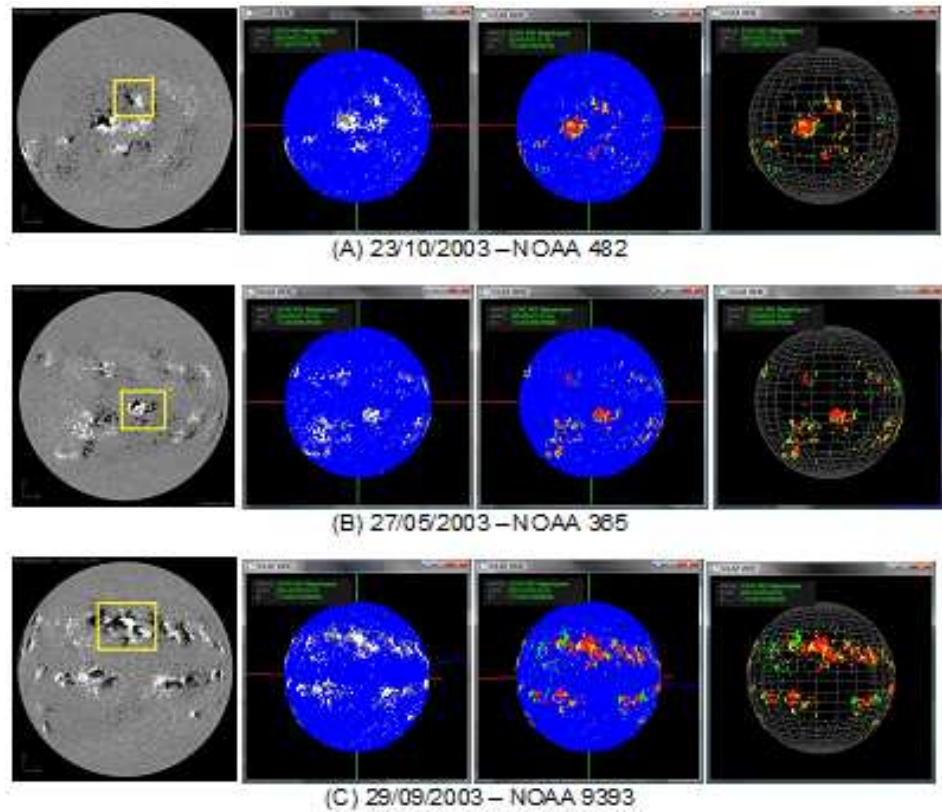


Figure 11. For each group, the 1st image is a magnetogram image, with the active regions under investigation surrounded by a yellow square, as a reference point, so it can be compared with the related images in the group. The 2<sup>nd</sup> image present active regions in 3D colour map. The 3<sup>rd</sup> image presents magnetic complexity regions. The 4<sup>th</sup> image shows the solar disk in the 3<sup>rd</sup> image in wired view.

Omar is currently a full-time PhD student working in the field of automated detection and tracking of solar features and solar activities prediction. He received his Higher National Diploma in Software Development from Bradford College and graduated from Bradford University with a first class B.Sc honors degree in Software Development Applications in 2007. His research interests include; space weather, digital image processing, applications development, and machine learning.

Author Photos (black-and-white passport size)  
[Click here to download high resolution image](#)

